AD-A065 859 FOREIGN TECHNOLOGY DIV WRIGHT-PATTERSON AFB OHIO F/G 20/7
ON THE FORMATION OF PRECISION BEAMS IN MULTISECTION LINEAR ELEC--ETC(U)
NOV 77 V I ARTEMOV, I A GRISHAYEV, I N GUGEL'

UNCLASSIFIED FTD-ID(RS)T-1919-77 NL

| OF |
ADA
065859

END
DATE
FILMED
4-79
DDC

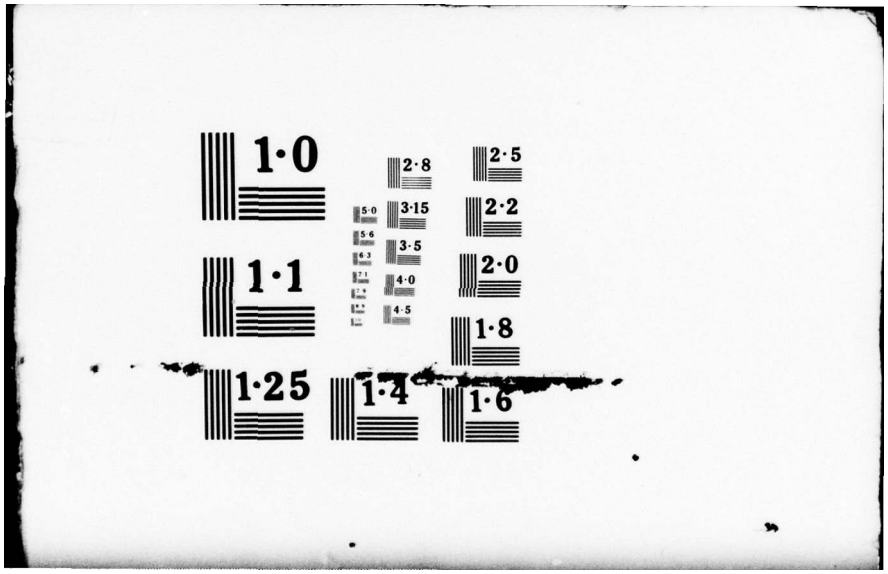
1·0
1·1
1·25
1·4
1·6
1·8
2·0
2·2
2·5
2·8
3·15
3·5
4·0
4·5
5·0
5·6

FTD-ID(RS)T-1919-77

FOREIGN TECHNOLOGY DIVISION

(1)

ON THE FORMATION OF PRECISION BEAMS IN MULTISECTION LINEAR ELECTRON ACCELERATORS

by

V. I. Artemov, I. A. Grishayev, et al.

Approved for public release; distribution unlimited.

UNEDITED MACHINE TRANSLATION

FTD-ID(RS)T-1919-77 2 November 1977

MICROFICHE NR: FTD-77-C-001391

ON THE FORMATION OF PRECISION BEAMS IN MULTISECTION LINEAR ELECTRON ACCELERATORS

By: V. I. Artemov, I. A. Grishayev, et al.

English pages: 43

Source: Ordena Lenina Akademiya Nauk USSR Ordena Lenina Fiziko-Tekhnicheskiy Institut, Khfti 71-31, Khar'kov, 1971, pp 1-30.

Country of origin: USSR
This document is a machine translation.

Requester: FTD/ETDP
Approved for public release; distribution unlimited.

PREPARED BY:

TRANSLATION DIVISION
FOREIGN TECHNOLOGY DIVISION
WP-AFB, OHIO.

U. S. BOARD ON GEOGRAPHIC NAMES TRANSLITERATION SYSTEM

Block	Italic	Transliteration	Block	Italic	Transliteration
А а	*А а*	A, a	Р р	*Р р*	R, r
Б б	*Б б*	B, b	С с	*С с*	S, s
В в	*В в*	V, v	Т т	*Т т*	T, t
Г г	*Г г*	G, g	У у	*У у*	U, u
Д д	*Д д*	D, d	Ф ф	*Ф ф*	F, f
Е е	*Е е*	Ye, ye; E, e*	Х х	*Х х*	Kh, kh
Ж ж	*Ж ж*	Zh, zh	Ц ц	*Ц ц*	Ts, ts
З з	*З з*	Z, z	Ч ч	*Ч ч*	Ch, ch
И и	*И и*	I, i	Ш ш	*Ш ш*	Sh, sh
Й й	*Й й*	Y, y	Щ щ	*Щ щ*	Shch, shch
К к	*К к*	K, k	Ъ ъ	*Ъ ъ*	"
Л л	*Л л*	L, l	Ы ы	*Ы ы*	Y, y
М м	*М м*	M, m	Ь ь	*Ь ь*	'
Н н	*Н н*	N, n	Э э	*Э э*	E, e
О о	*О о*	O, o	Ю ю	*Ю ю*	Yu, yu
П п	*П п*	P, p	Я я	*Я я*	Ya, ya

*ye initially, after vowels, and after ъ, ь; e elsewhere.
When written as ё in Russian, transliterate as yё or ё.

RUSSIAN AND ENGLISH TRIGONOMETRIC FUNCTIONS

Russian	English	Russian	English	Russian	English
sin	sin	sh	sinh	arc sh	$\sinh^{-1}$
cos	cos	ch	cosh	arc ch	$\cosh^{-1}$
tg	tan	th	tanh	arc th	$\tanh^{-1}$
ctg	cot	cth	coth	arc cth	$\coth^{-1}$
sec	sec	sch	sech	arc sch	sech^{-1}
cosec	csc	csch	csch	arc csch	csch^{-1}

Russian	English
rot	curl
lg	log

V.
I. Artemov, I. A. Grishayev, I. N. Gugel', G. K. Dem'yanenko, A. N. Dovbnya, Ye. V. Korniyenko, N. I. Mocheshnikov, F. A. Peyev, V. V. Petrenko.

ON THE FORMATION OF PRECISION BEAMS IN MULTISECTION LINEAR ELECTRON ACCELERATORS.

Page 2.

Is described the method of obtaining precision beams linear electron accelerator, based on the use cf communication/connection of radial and phase motion. Is investigated the effect of high-frequency and current instabilities on the parameters of beam. Is set forth the procedure of the measurement of the emittance of beam at output of accelerator to 2 GeV. During measurement was utilized the plate with the set of narrow slots and detector. Are compared the experimental characteristics of beam with calculated.

In obtaining precision beams on linear accelerators significant role it plays the questions of optics both in the accelerating channel and in the different systems of formation and transportation of particles. The optical properties of multisection linear accelerator to a high degree depend on the various kinds of the perturbing forces, which exist in the real accelerating channel, and also on the properties of the system of beam focusing on accelerator. The fundamental characteristics of beam at output of accelerator (energy spectrum, current, emittance) in many respects are determined also by the value of the phase volume of the beam of injector-accelerator.

In multisection linear accelerator 2 GeV in energy between transverse and axial motions there is communication/connection [1], caused by the presence in the accelerating structures of transverse high-frequency fields and by the chromatic aberrations of the system of beam focusing. This communication/connection leads to the three-dimensional/space separation of particles with the different phases in horizontal plane, which in principle makes it possible to create sufficiently narrow phase channel by means of the irising of beam in the appropriate places of accelerator. The creation of sufficiently narrow phase channel (phase collimation) would give not

only and the monochromatization of the accelerated beam, but also substantially it would decrease its effective emittance.

I. System of the phase collimation of beam.

The existed system of beam focusing provided the greatest separation of particles into the phases during simultaneous satisfaction of the conditions of stagmatic focusing in the area of 20-th accelerating sections.

Page 4.

The experiments, carried out with the adjustable collimator on 20-th sections, they showed the clear dependence between the size/dimensions of the target/purpose of collimator and the width of the energy spread of beam at output of accelerator [2]. The role of this collimator is analogous to the role of collimator-monochromator at the output/yield of magnetic analyzers. As in the systems of transportation, an improvement in the quality of beam during phase collimation is reached, at first glance, because of the loss of the intensity of the accelerated current. In actuality, the situation will press otherwise. Since at present the output current is

determined by the threshold of the emergence of lateral instability [3], which is much less than the current of injector-accelerator, creation of narrow phase channel at the very beginning of accelerator must not bring to a decrease in the accelerated current.

The searches for the accelerating channel in which would be accelerated "pure/clean" beam with a small phase extent of cluster they led us to the diagram which was shown in Fig. 1.

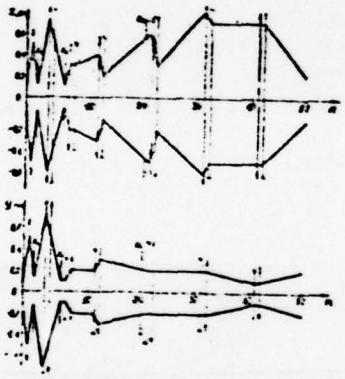

Fig. 1. Envelopes of particles.

In this figure are shown the envelope of particles in horizontal (x) and vertical (y) planes, and also the arrangement of magnetic quadrupole lenses and collimators k_1, k_2, k_3. Lens L_1 and collimator k_1 produce the preliminary selection of particles on the phases of injector beam, utilizing certain communication/connection between energy of particle and phase in the output/yield of injector-accelerator.

The focussed beam of the determined energy to the slot of collimator k_1, it is possible to create the most favorable conditions for the passage of particles only with the determined phase set, since the particles of other energies, but, therefore, and with another phase set, will have the larger size/dimension of beam in collimator k_1. During further particle motion in the accelerating sections communication/connection between energy of particle and phase becomes more explicit, energy of particle is the function of location of its relative to wave crest. Therefore the parameters of the doublet of quadrupole lenses - L_2, L_3 and collimators - k_2 must be selected from the condition of the preferred incidence/impingement in the slot of particles, arrange/located on wave crest. Let us examine in more detail the procedure of the selection of these parameters. Let us introduce the following designations:

M_x, M_y - the matrix/die of the doublet of quadrupole lenses respectively in horizontal and vertical plane;

L_i is a matrix/die of the transition of the i free interval/gap;

M_i - the matrix/die of the transition of the i accelerating

section (since in the first four sections are used the symmetrized matchers, matrix/die M_i it will be double-row and identical both in vertical and in horizontal plane).

Page 6.

The complete matrix/die of transition from collimator k_1 to collimator k_2 can be written as

$$\left.\begin{aligned} M_x &= T_2 M_x T_1 \\ M_y &= T_2 M_y T_1 \end{aligned}\right\}, \qquad (I)$$

where

$$T_1 = M_2 L_2 M_1 L_1, \quad T_2 = L_4 M_4 L_3 M_3.$$

Matrix/dies T_1, T_2 take the form:

$$T_1 = \begin{pmatrix} 1 & l_1(\varphi) \\ 0 & \alpha_1(\varphi) \end{pmatrix}; \quad T_2 = \begin{pmatrix} 1 & l_2(\varphi) \\ 0 & \alpha_2(\varphi) \end{pmatrix}, \qquad (2)$$

where

$$l_1(\varphi) = L_1 + \frac{E_0}{q\mathcal{E}\cos\varphi + dE_0} \ln\frac{E_1}{E_0}\, e^{\alpha l} + \left[L_2 + \frac{E_1}{q\mathcal{E}\cos\varphi + dE_1} \ln\frac{E_2}{E_1}\, e^{\alpha l}\right]\frac{E_1}{E_2}$$

$$l_2(\varphi) = \frac{E_2}{q\mathcal{E}\cos\varphi + dE_2} \ln\frac{E_3}{E_2}\, e^{\alpha l} + \frac{E_2}{E_3} L_3 + \frac{E_2}{E_3}\left(\frac{E_3}{q\mathcal{E}\cos\varphi + dE_3} \ln\frac{E_4}{E_3}\, e^{\alpha l} + \frac{E_3}{E_4} L_4\right)$$

E_i - energy of particle at the output/yield of the i section;

E_0 is energy injection;

$q\mathcal{E}$ - the strength of field in the beginning of section;

α is decay constant of field in section;

Z - the length of section;

$$\alpha_1(\varphi) = \frac{E_0}{E_2}; \quad \alpha_2(\varphi) = \frac{E_2}{E_4}.$$

Matrix/dies M_x, M_y in the approach/approximation of the thin lenses

$$M_x = \begin{pmatrix} 1 & \frac{L}{F_1(\varphi)} ; & L \\ -\frac{1}{F_1(\varphi)} + \frac{1}{F_2(1-\frac{L}{F_1})} ; & 1 + \frac{Z}{F_2(\varphi)} \end{pmatrix}$$

$$M_y = \begin{pmatrix} 1 + \frac{L}{F_1} , & L \\ -\frac{1}{F_1(\varphi)} - \frac{1}{F_2}\left(1 + \frac{L}{F_1}\right) ; & 1 - \frac{Z}{F_2(\varphi)} \end{pmatrix} \qquad (3)$$

where $F_1(\varphi)$, $F_2(\varphi)$ - the focal lengths of the first and second lens; L - the distance between lenses. By substituting in (1) expressions for matrix/dies to (2) and (3) and after requiring

satisfaction of the conditions of stigmatic focusing simultaneously in horizontal and vertical plane at the entrance into collimators ($k_2, \{(R_{12})_x = (R_{12})_y = 0\}$) we will obtain the single-valued relation between the parameters of focusing and the size/dimensions of the collimators:

$$\frac{F_1}{F_2} = \frac{l_1}{l_2}\,\frac{L+l_2}{\alpha_1 L + l_1} \qquad (4)$$

$$F_2 = l_2 \sqrt{\frac{L^2\alpha_2 L + l_1^2}{(L+l_2)[l_1 - \alpha_1(L+l_2)]}}$$

Page 7.

With a radius of collimator k_1, equal to r_c that part of the cluster, which is accelerated on wave crest, in the region of collimator k_2 has the transverse size/dimensions

$$x_{min} = \left\{1 + \frac{L}{F_1} + l_2\left[\frac{1}{F_1} - \frac{1}{F_2}\left(1 + \frac{L}{F_1}\right)\right]\right\} r_c$$

$$y_{min} = \left\{1 - \frac{L}{F_1} + l_2\left[\frac{1}{F_2}\left(1 - \frac{L}{F_1}\right) - \frac{1}{F_1}\right]\right\} r_c \qquad (5)$$

For particles with other phases, as a result of the difference in energies, the condition of stigmatic focusing is not satisfied, therefore, transverse size/dimensions they exceed x_{min} and y_{min}.

Therefore, if we select the size/dimensions of collimator k_2 from condition (5), then this system will fulfill the functions of the separator of particles through the phases with separation ratio, equal to

$$k(\varphi) = \frac{\Delta S_x(\varphi)}{S_x} \cdot \frac{\Delta S_y(\varphi)}{S_y} \cdot \rho(\varphi), \qquad (6)$$

where S_x - the emittance of beam in x-plane;

S_y - the emittance of beam in y-plane;

ΔS_x, ΔS_y is part of the emittance of beam, included in the intervals, given by formula (5);

$\rho(\varphi)$ - the normalized function of particle distribution according to phases (for uniform distribution $\rho(\varphi) = 1$).

Beginning from the fifth section, for radial motion is exerted a substantial influence transverse high-frequency fields in matchers. The matrix/die of the transition of section in horizontal plane depends now on phase not only through its communication/connection with energy, but also directly; therefore it becomes triple:

$$\begin{pmatrix} x \\ x' \\ y \end{pmatrix} = \begin{pmatrix} 1 & \widetilde{L}_n & \widetilde{L}_n \frac{a}{E_n} \\ 0 & \frac{E_n}{E_{n+1}} & \frac{a(1+e^{-d2})}{E_{n+1}} \\ 0 & 0 & 1 \end{pmatrix}, \qquad (7)$$

where $a = \int \varepsilon_\perp(z)\, dz$, $\varepsilon_\perp(z)$ - cross field in matcher.

Page 8.

The identification of the parameters of quadrupoles in the interval/gap between ~~5-1~~ 5th and ~~20-1~~ 20th sections was conducted by the method of random search on EVM [computer]. The minimized functional of the quality of beam took outer limits during simultaneous satisfaction of the condition of stigmatic focusing on collimator k_3 and the absence of the losses of particles ($\varkappa_2 \varkappa_2$, $\varkappa_2$ - the aperture of accelerator) with phase $\varphi = 0$. Figure 2 depicts the emittances of beams of particles with different phases in collimators k_2 and k_3, and also particle distributions according to phases after the phase collimation, calculated taking into account the function of particle distribution according to the phases of used injector accelerator [4].

Thus, the system of phase collimation in the absence of the various kinds of fluctuations must provide beam at output of accelerator with energy spread $\frac{\Delta E}{E} \leq 0{,}2\%$ on basis/base.

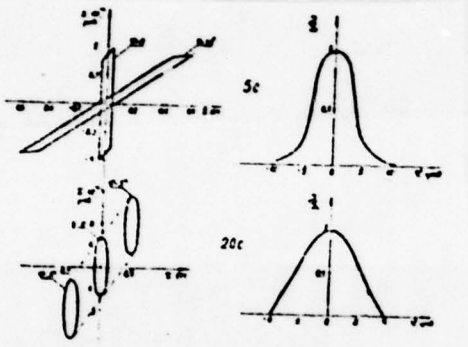

Fig. 2. Emittance of beam and the function of particle distribution according to the phases afterward 5 and of 20 sections.

[c = s]

II. Effect of fluctuations on the parameters of the accelerated beam.

The experimental studies of narrow phase channel showed that the parameters of beam at output of accelerator do not correspond

calculated. To the reason for this nonconformity it consists in the effect of the high-frequency fluctuations of accelerating field by the parameters of beam, which were not considered in the given above calculations. The effect of high-frequency fluctuations of the parameters of the beam of linear accelerator were studied earlier in some works, in particular in [5]. However, in this case it was assumed that the radial motion virtually is equal for all particles in the accelerated cluster. In our case this assumption is not justified. Due to communication/connection transverse and phase motion.

For the explanation of the effect of fluctuations on the parameters of beam we have investigated statistical properties of instabilities and communication/connection between them. Of the fluctuations of the parameters it is possible to break into two groups: slow, from one momentum/impulse/pulse to the next (current of injector, the currents of correction and quadrupole lenses), and rapid, during momentum/impulse/pulse (change in the frequency and amplitude on each accelerated section). Were investigated three forms of the instabilities: current, amplitude and frequency. Figure 3 depicts the oscillograms of amplitude and frequency during momentum/impulse/pulse on 19-th accelerating sections. Statistical processing was conducted according to 35 working sections with the selection through 0.1 microseconds. Figure 4 shows the distribution

function of phase fluctuations at the moment of time τ = 0.7 s. The dependence of the standard deviations of the phase of slip and amplitude, and also the mathematical expectation of these parameters from time it is shown in Fig. 5 and Fig. 6. The correlation analysis, carried out for the detection of linear communication/connection between σ_φ and m_φ, σ_ξ and σ_η, m_η and m_ξ and also between the given variables time became the following results. The correlation coefficients between the enumerated variables are close to zero. Maximum value reaches the linear correlation coefficient between σ_φ and time and composes value 0.06. Therefore during the simulation of high-frequency fluctuations on computer it was considered that between the fluctuations of frequency and amplitude is absent any communication/connection.

Page 10.

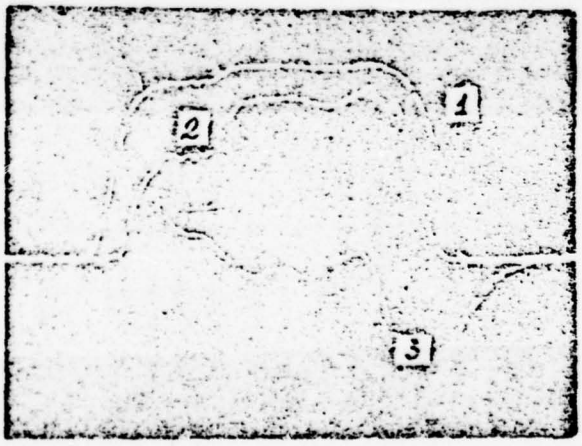

Fig. 3. Characteristic amplitude (2) and frequency (3) fluctuations on the accelerating section.

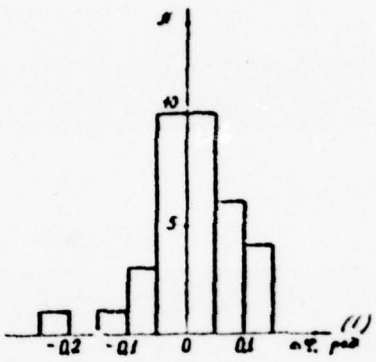

Fig. 4. The distribution function of frequency fluctuations on accelerator, expressed in the phases of slip, during τ = 0.7 ms.

Key: (1). rad.

Page 11.

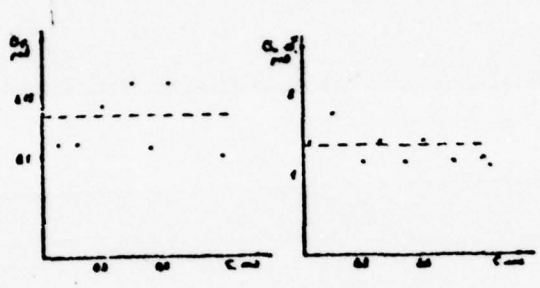

Fig. 5. Dependence of the standard deviations of phase (σ_φ) and amplitude (σ_a) fluctuations from time.
[pa∂ = rad]

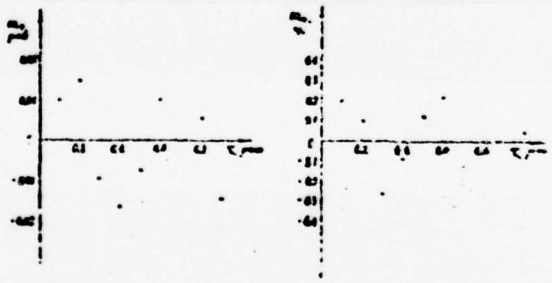

Fig. 6. Dependence of the automatic expectation of phase (m_φ) and amplitude (m_a) instabilities on time.
[pa∂ = rad]

Page 12.

The standard deviations of frequency and amplitude in time in this case were set/assumed by constants, but mathematical expectations m_φ and m_a in view of their low value were accepted equal to zero. This proposition is substantiated, since statistical portrait we attempt to construct from sufficiently small sample from general population of fluctuations. The distribution function of amplitude and phase fluctuations was described by the law of Gauss with rms deviation respectively

$$\sigma_\varphi = 0{,}14 \text{ rad}, \quad \sigma_a = 1{,}35\%.$$

The instabilities of the value of the current of injector were considered evenly distributed in range of ±5o/o from the value of the rated current, equal to 20 mA. In Fig. 7 are presented the results of simulation on to the Monte-Carlo method the combined effect of the enumerated down fluctuations on the parameters of beam. For a comparison Fig. 8 depicts the experimentally obtained spectrum for the standard operating mode 1 GeV in energy after the creation of the system of phase collimation.

From the results of this work it follows that the ways of phase collimation it is possible to create on linear multisection

accelerator the narrow phase channel, which makes it possible to obtain at the output/yield of accelerator precision beams with energy homogeneity better than 0.1o/o on basis/base. In this case several times decrease the emittances of beam. However, the presence of fluctuations it expands phase channel, in consequence of which the parameters of beam at output of accelerator they deteriorate: grow/rises the energy spread to 0.5o/o, the emittances of beam increase 2-3 times.

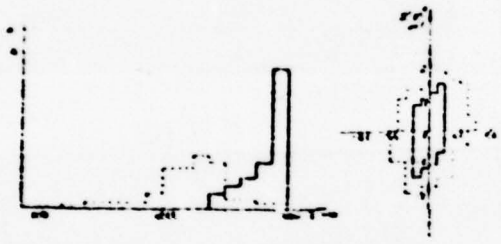

Fig. 7. Effect of fluctuations on the parameters of the accelerated current (energy spectrum and the emittance of beam).

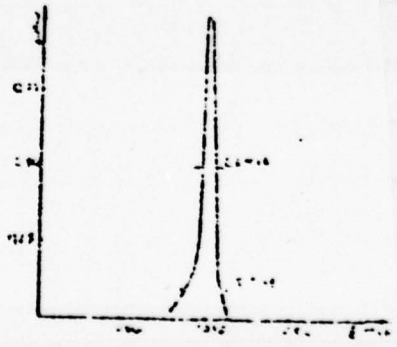

Fig. 8. Experimental spectrum of the accelerated particles at the output/yield of accelerator during phase collimation.

III. Characteristic measurement of beam.

one of the important parameters of beam at output of accelerator is emittance [6]. The information about the value and form of emittance at the output/yield of accelerator makes it possible to solve the problem of the transportation of beam to target with the minimum losses and optimally. In a number of cases of the condition of experiment are set the limitations on the value of emittance, is sometimes necessary the operational information about value to the form of the emittance of beam. Furthermore, the emittance is the good diagnostic parameter of accelerator, since to value and its form they depend on energy of the accelerated beam, level frequency-phase instability on the cell/elements of high-frequency system, phase width of cluster, tuning of the focusing channel, etc. Consequently, for the most effective use of a beam of accelerator and optimization of the conditions of experiment is necessary the measurement of value and form of the emittance of beam on accelerator.

During the measurement of emittance at the output/yield of accelerator to 2 GeV at the basis of procedure were placed the methods, described in the literature [7, 8, 9], taking into account our specific conditions. Common/general/total for all these methods is the use of a plate with the set of slots, adjustable in the path of beam for the isolation/liberation of its parts, and also detector for determining the size/dimension of the beam, adjustable at certain flight path from plate and intended for determining the range of angular deflections in beam.

RESEARCH EQUIPMENT.

The location of equipment during the measurement of emittance at the output/yield of accelerator to 2 GeV is schematically shown in Fig. 9. Between initial accelerating section I and rotary magnet 2, it is establish/installed to plate with the set of slots 3. On the flange of straight line the output/yield is fastened cassette 4 with glass specimen/sample 5.

Plate with the set of slots is made on tantalum 2 mm thickness. The location of target/purposes illustrates Fig. 10. Distance between the target/purposes of desirable having minimum in order to ensure obtaining information about divergence at a great many points. However, the value of this distance is limited by need sufficient clear separation of the impressions of parts of the beam, passed by target/purposes, on detector, the number of slots and their height/altitude are selected so that the size/dimensions of the working section of plate would be knowingly more than the size/dimensions of beam. With the thickness of tantalum plate 2 mm and of energy of electrons 1000 MeV rms scattering angle of particles, striking the slit is approximately $4 \cdot 10^{-3}$ radians. Together with secondary particles the scattered electrons form on glass the weak background, on which clearly are isolated the impressions of parts of the beam, passed by the slots. The displacement/movement of plate is conducted remotely; under beam can be introduced the set of vertical or horizontal slots. To plate with slots is separated from detector by drift interval/gap 4.5 m long.

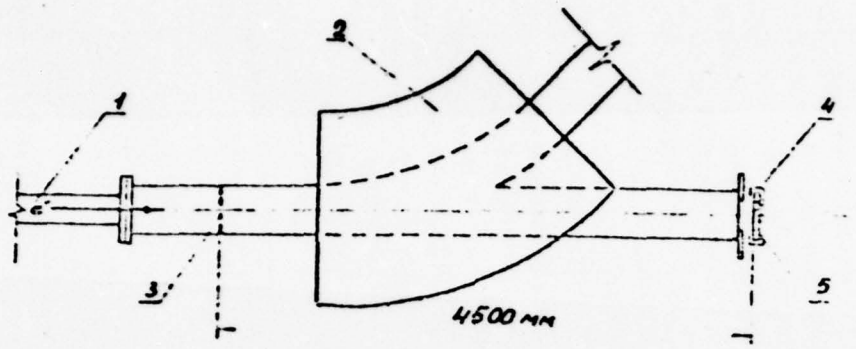

Fig. 9. Location of equipment with measurement of emittance at the output/yield of accelerator to 2 GeV.

Page 16.

Conducting of measurements is complicated by the facts that the electron conductor of drift section passes through the clearance of rotary magnet. It is natural that during the measurement of emittance the magnetic intensity in magnet gap must be sufficiently small. Therefore during the time of the measurement of emittance the residual field is compensated with the aid of an additional winding so that the value of its strength would not exceed several gauss. The error introduced in this case does not exceed $\gamma = \pm 0.05$ mm, to $\gamma' = \pm 0.5 \cdot 10^{-3}$.

The drift gap terminates in a flange, on which in the place of the passage of beam is establish/installed the copper foil with a thickness of 50 microns. Close to flange is attached the cassette, controlled remotely, in which simultaneously it can be charged 10 glass specimen/samples. During the measurements alternately they are establish/installed under beam, making it possible to obtain the operational information about changes in the emittance. Time for the replacement of plate does not exceed 5 s.

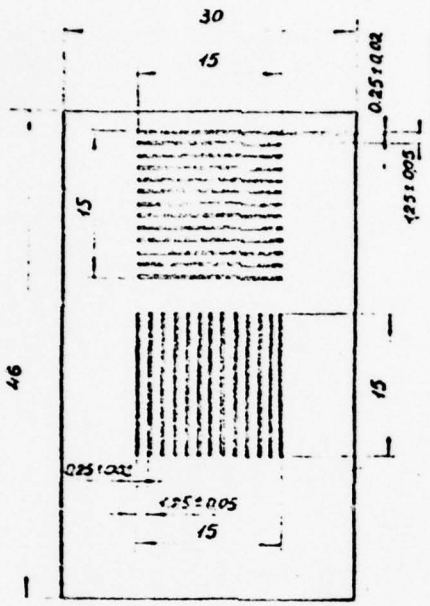

Fig. 10. Plate from tantalum with the set of vertical and horizontal slots.

Page 17.

As the detector of beam is utilized sheet of glass GOST [All-union State Standard]-III-65 by thickness 2.7 mm with size/dimension of plates 45 x 45 mm. The reason for the selection of glass were the following considerations. The measurement of emittance during the use of this procedure assumes as one of the operations of determination of the size/dimensions of parts of the beam, passed by

slots. However, in such cases when the transverse size/dimensions of beam compose value on the order of 0.5 — 1.5 mm. many methods of the measurement of the airfoil/profile of beam they encounter difficulties. For this purpose can be used the change in the transparency of the glass, caused by effect of radiation [10]. Research on the dependence of the coefficient of transmission [11] on the intensity of beam with the thickness of glass 2.7 mm and the energy of electrons of approximately 1000 MeV showed that can be measured the particle densities from $5 \cdot 10^9$ to $2 \cdot 10^{12}$ e/per 1 mm^2.

The exposure time of glass depends on the intensity of beam and is selected in such a way that the coefficient of transmission and the quite dense place would be about 10o/o. In this case is provided a greatest quantity of gradations of the coefficient of transmission.

The total time necessary for preparation and to the measurement of emittance, is 5-8 minutes. The duration of exposure with the working values of the current of accelerator (0.1-1 μA) vary within the range of 1 to 10 s.

PROCESSING RESULTS.

The impressions of beam in glass specimen/sample, obtained during the measurement of horizontal emittance, are represented in Fig. 11.

Fig. 11. Impressions of beam on the glass plate during the measurement of horizontal emittance.

Paage 18.

In each of the replicas the positicn of particles on horizontal is assigned by coordinate x+x'L, where x is a coordinate of the corresponding slot, x' is a value of the divergence of beam, L - distance from plate with slots of detector. Subsequently of value x+x'L let us designate X.

For the photometric measurement of the impressions of beam in glass specimen/sample was used the microphotometer MF-4 whose construction makes it possible to produce the notation of the values of the coefficient of transmission for photographic materials during the automatic displacement/movement of object table. The width of measuring slot, i.e., its size/dimension in the direction of photometric measurement is selected as being equal to 0.003 mm, the height/altitude of measuring slot is limited by the construction of

microphotometer and it is 3.3 mm, the height/altitude of measuring slot is limited by the construction of microphotometer and it is 3.3 mm. The size/dimension of impressions in the majority of cases exceeds the height/altitude of measuring slot; therefore the notation of the values of the coefficient of transmission was conducted several passages with the displacement of measuring slot on height/altitude so that the boundary of the examine/scanned by photometer zones would coincide and impressions were completely photometrically scanned. The notation of the values of the coefficient of transmission for the impressions, shown Fig. 11 gives in Fig. 12.

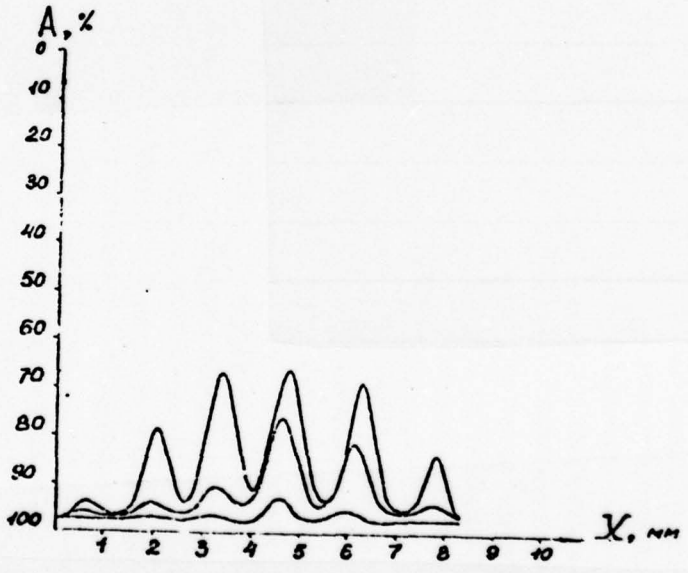

Fig. 12. Notation of the values of the coefficient of transmission for the impressions of Fig. 3 obtained on microphotometer MF-4.

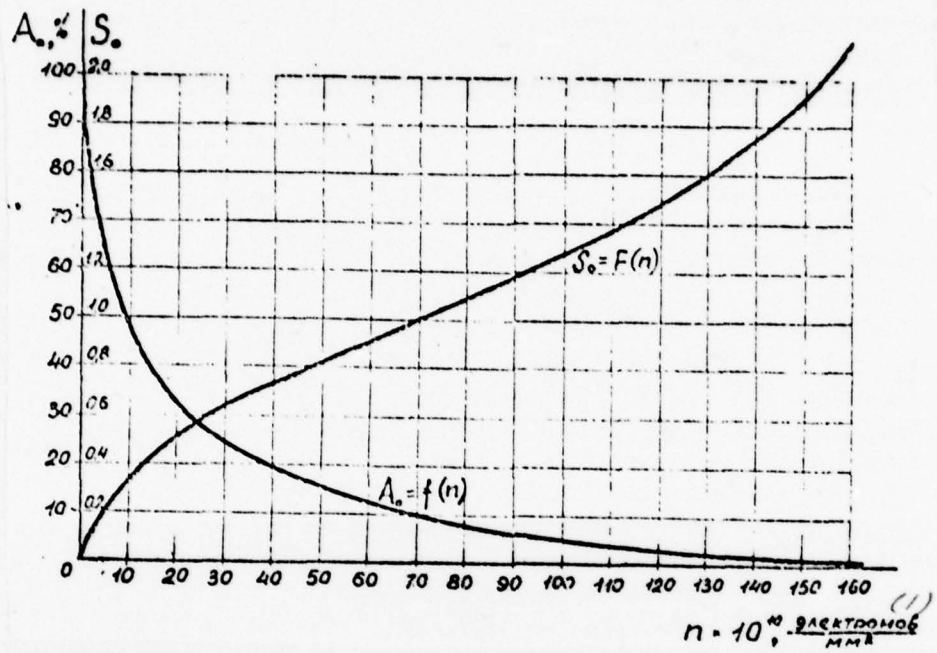

Fig. 13. Calibration curves for glass sheet GOST- III-65 (δ = 2.7 mm) with energy of the accelerated beam E = 1000 MeV.

Key: (1). electrons/mm².

Page 20.

Then is conducted the recalculation of the coefficient of transmission and the value of specific particle density on 1 mm² for all values of X. For a recalculation was utilized calibration curve (Fig. 13).

The specific particle density on 1 mm² of the surface of specimen/sample is the function of coordinates X and Y and can be designated in m (X, y). Integration m (X, y) for y for each this value of X makes it possible to pass to the density of distribution of particles along the axis X

$$\int m(X,y)\,dy = M(X) \qquad (I)$$

Taking into account the fact that with photometric measurement occurs the averaging of the coefficient of transmission in the area of measuring target/purpose, the operation of integration was replaced for each coordinate X by the addition of three (according to the number of curve/graphs) values of specific particle density with the subsequent multiplication of the sum by the height/altitude of measuring slot of mm. The obtained in this case curve/graph of the density distribution of particles along the axis X is represented in Fig. 14. This curve/graph makes it possible to produce the calculation of divergence for each spot after separation of background and deposition of the diaphragming slots.

The isolation/evolution of the background, caused by the scattered on tantalum plate particles, is necessary for jogging of the zero values M (X) on the boundaries of spots. The deposition of the location of the diaphragmed slots (see Fig. 14) makes it possible to determine zero values x'ℓ for each spot and to pass on the

calculation of the values of divergence on the boundaries of spots. These values, calculated as quotient $\frac{x'}{x}$ with the appropriate sign, determine angular extent of beam, isolated by each slot, and together with the appropriate value of x they are points on the boundary of the emittance of beam on plane x, x'. Similar calculations, produced for all spots, make it possible to determine the boundaries of the emittance of Fig. 15. This emittance corresponds 100o/o of particles in beam.

The practice of the measurement of the emittance of beams shows that the particle distribution in two-dimensional phase space is nonuniform. Because of this the emittances of entire beam and its nucleus, which includes 80-90o/o of particles, differ 2-2.5 times. The measurement of the emittance of the nucleus of beam and determination the corresponding to it part of total current was conducted with the application/use of the following procedure.

Page 21.

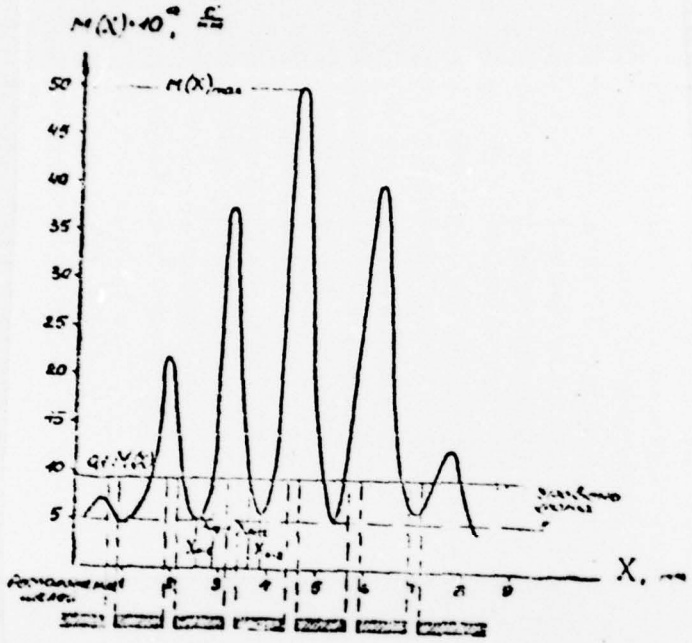

Fig. 14. Density distribution of particles along the axis X.

Key:[Keys are illegible.]

Page 22.

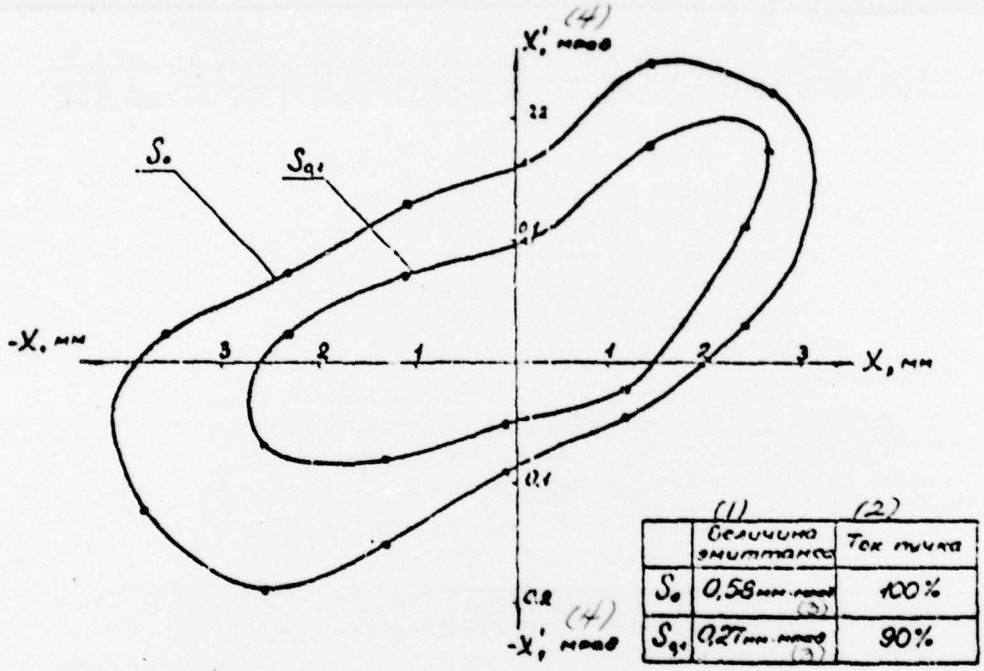

Fig. 15. Emittance of the beam of the accelerated electrons, by measured at the different levels M (X).

Key: (1). Value of emittance. (2). Beam currents. (3). mm•mrad. (4) mrad.

If we in Fig. 14 in parallel to X-axis conduct the line, which corresponds 10o/o of the maximum value M (X), then in the points of the intersection of curve/graphs M (X) with this line will be obtained the points, which determine the new boundary of emittance.

The portion of particles, characterized by emittance, was determined as follows. In the examination of function M (X) for one spot it is easy to note that the total quantity of particles, passing through this slot, and designated $n(x)$, can be determined by the integration

$$\int_{X_{o.1}}^{X_{o.2}} M(X)\,dX = n(x). \qquad (2)$$

where $X_{o.1}$ and $X_{o.2}$ - value X on the boundaries of the spots, with which function M (X) takes zero values.

Value $n(x)$ characterizes at the same time the density of distribution of particles according to x in transverse beam section in the location of the slot in question. The set of values $n(x)$, obtained during integration M (X) for different spots, makes it possible to construct the curve/graph of the density distribution of

particles according to x in the beam being investigated. Integrating $n(x)$, we obtain the total quantity of particles in beam N.

$$\int_{-\infty}^{+\infty} n(x)\,dx = N \qquad (3)$$

Or, by utilizing expression (2), it is possible to write

$$\int_{-\infty}^{+\infty} dx \int_{\lambda_{o1}}^{\lambda_{o2}} M(X)\,dX = N \qquad (4)$$

The calculation of a quantity of particles for the emittance, determined at the level 10o/o of the maximum value M (X), is conducted similarly. Difference lies in the fact that a quantity of particles N_{o1} is computed in accordance with the expression

$$\int_{-\infty}^{+\infty} dx \int_{\lambda_{o1}}^{X_{o1-2}} M(X)\,dX = N_{o1}, \qquad (5)$$

where X_{o1-1} and X_{o1-2} are values X on the periphery of the spots, by which $M(X)=0, M(X)_{max}$.

Page 24.

The results of measurements, processed with the aid of the described procedure, are represented in Fig. 15.

ERRORS DURING THE MEASUREMENTS OF EMITTANCE.

During the measurement of emittance by the means of plate with the set of slots there are following sources of errors. This first of all the error in the determination of form and value of emittance because of the limited quantity of measuring points. Divergence is measured only at those points of the cross section, where the beam it passes through slots, and the information about intermediate points it is lost. For this reason desirable would be to make the distance between slots minimum; however, one should consider the need for the clear separation of spots on detector. The error indicated is laid in the very nature of method. It can be decreased by the repeated measurement of emittance with the intermediate displacements of beam along this axis by low value and of the subsequent comparison of results.

Is possible also the fault of measurement of divergence, determined by the width of the measuring slot of photometer. With the width of slot 0.003 mm and basis 4.5 m this error composes $\sim 1 \cdot 10^{-4}$ radians.

The use of glass and the quality of detector has a series of the special feature/peculiarities, which must be considered during measurements, for example, necessary to eliminate the effect of scattering electron beam and the substance of glass from the results of measurements. The authors produced the estimation of the measurement of the size/dimension of the beam with of its passage through glass. It is establish/installed that with energy of electrons 1000 MeV and during use for the measurements of glass 2.7 mm thickness the scattering does not affect the accuracy of results.

It should be noted that irradiated glass in the course of time is provided. This process is developed unevenly in time and its speed depends on radiation dose at the particular point. Therefore produced the measurement of the dependence of the coefficient of transmission on time after irradiation for the different initial values of coefficient, which made it possible to introduce the appropriate corrections during processing the results of measurement.

The accuracy of measurements during the use of the described method is determined also by the sensitivity of photometer, by the magnitude of error during removal/taking calibration curve and by the deviation of the thickness of glass from rating.

The macrophotometer MF-4 provides the accuracy of the measurement of the coefficient of transmission not worse than 1o/o. Error during removal/taking curve does not exceed 5o/o a is caused mainly by error during the measurement of exposure and intensity of electron beam. According to GOST-111-65, the deviation of the thickness of glass from rating is ±0.2 mm. However, measurement of the thickness of glass specimen/sample in each case made it possible to introduce the appropriate correction, assuming that the photographic density was proportional to the thickness of glass. The effect of changes in the chemical composition of the different party/batches of glass for a change in the coefficient of transmission noticed was not.

Taking into account corrections, the random rms error, calculated after five-fold measurement of the emittance of one beam, was ±10o/o with probability 0.95.

SOME RESULTS OF THE MEASUREMENT OF EMITTANCE ON ACCELERATOR 2 GeV

With the use of the described procedure a series of the measurements of emittance during the different mode/conditions of work of the accelerator.

Figure 16 shows the curve/graphs of current distribution in beam depending on the value of emittance. In this case the accelerator worked in one on standard mode/conditions. Energy of electrons at the output/yield of accelerator was equal to 1100 MeV with the width of spectrum 0.6o/o at the level of 0.1 maximum intensities. Beam current composed value 0.4 μA. The values of phase density for the horizontal and vertical emittances, measured at the level 0.1 M (X), are equal to with respect 1.35 [illegible] and 2.4 [illegible]. A difference in the radial- angular characteristics in planes xx' and yy' is explained by effect on the beam of transverse electric field in the matchers of accelerating sections [12]. The calculation of optics of accelerator for 2 GeV [13] showed that the existence of cross fields in sections in the presence of the system of focusing and clusters with the final phase widths leads to the appearance of an effect of the separation of particles into the phases in horizontal direction. According to the results of the calculation is carried out the investigation the dynamic loudspeakers of radial motion in accelerator.

For this was changed the optical diagram of the initial part of the accelerator: were introduced supplementary quadrupole lenses and diaphragms with alternating/variable opening/aperture to 3, 6 and 20-th accelerating sections. This made it possible to derive on particle accelerations, which were being located on the periphery of cluster, to decrease the emittance at the output/yield of accelerator and to raise the phase density of beam.

Since the effect of separation is most pronounced on 20-th sections, are given to results, relating to the dependence of horizontal emittance, beam current to the phase density of beam at output of accelerator on the size/dimension of the opening/aperture of diaphragm A for this section.

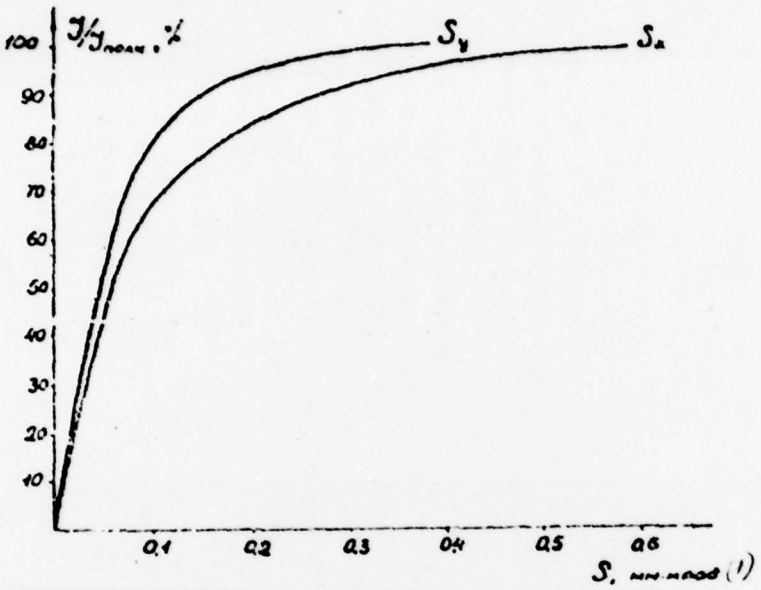

Fig. 16. Current distribution in beam depending on the value of emittance.

Key: (1). mm•mrad.

Page 27.

The corresponding curve/graphs are represented in Fig. 17.

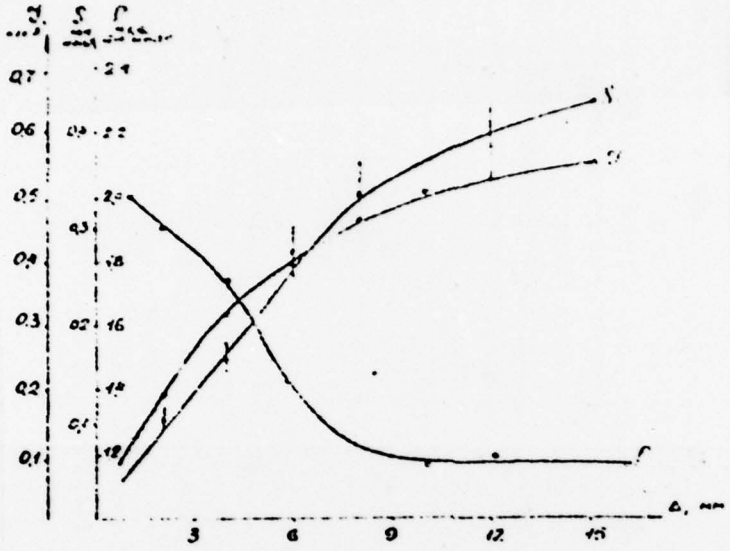

Fig. 17. Dependences of horizontal emittance, beam current and phase density of beam at output of accelerator on the size/dimension of the opening/aperture of diaphragm on 20-th sections.

Key: Keys are illegible.

Page 28.

As is evident, the phase density noticeably grow/rises during a decrease in the opening/aperture of diaphragm from 8 to 4 mm. The horizontal and vertical emittances of beam with Δ-4 mm are represented in Fig. 18.

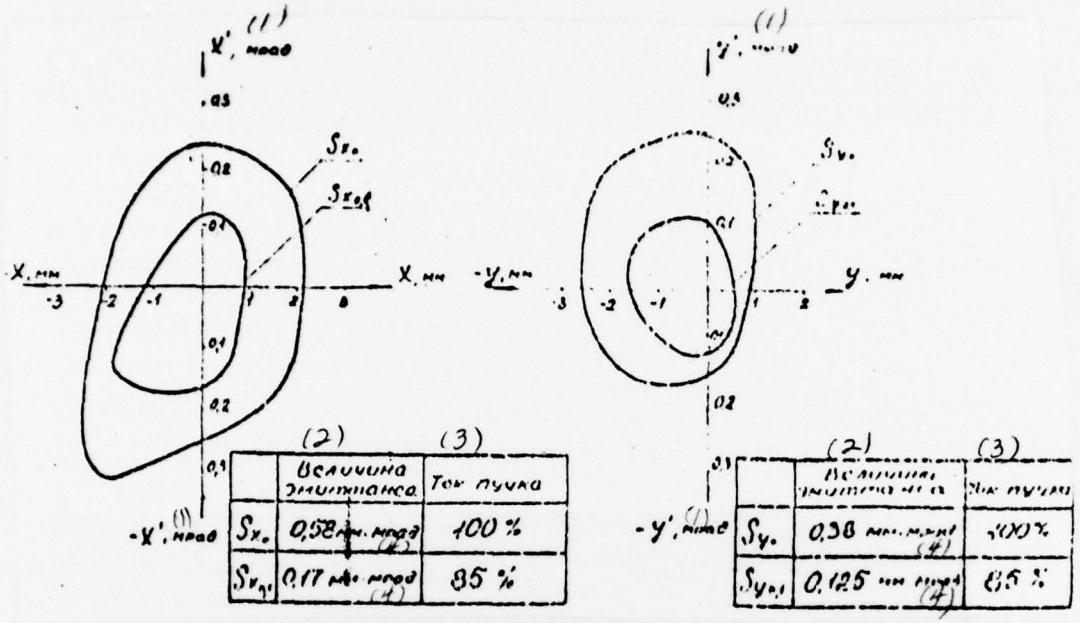

Fig. 18. Horizontal and vertical emittances of beam with the size/dimension of the opening/aperture of diaphragm on 20-1 sections Δ = 4 mm.

Key: (1). mrad. (2). Value of emittance. (3). Beam current. (4). mm·mrad.

Page 29.

REFERENCES

1. И.А.Гривцев,И.Н.Гугель,А.Н.Довбня,Н.И.Мочевников,В.В.Петренко.
   ХТФ, 41, № 4, 1971
2. Б.И.Артёмов, И.А.Гривцев, А.Н.Довбня, Н.И.Мочевников, В.В.Петренко. Доклад на II Всесоюзном совещании по ускорителям, Москва, 1970.
3. А.Н.Зимов, И.А.Гривцев, Г.Д.Кремской, Н.И.Мочевников.
   ХТФ, 38, № 1, 1968.
4. Е.К.Островский,А.Н.Зимов,Г.Д.Кремской,В.А.Свинцов.
   ПТЭ, № 4, 1968.
5. Г.П.Авраамов,А.В.Сальков. Сб."Ускоритель", Атомиздат,вып.XI, с.147, 1969.
6. А.Бамфорд. Транспортирование пучков заряженных частиц. Атомиздат, М., 1969.
7. Mc Keever, Yokoseva A., RSI, 33, № 7, p. 746-749, 1962
8. A.von Steenbergen, NIM, v.51, № 2, p.245-253, 1967.
9. R.J.Allison et al.,IEEE Trans.Nucl.Sci., 1969, v.16, № 3, p.11, 1055-1058.
10. G.E.Fisher, RSI, 35, № 8, p.1081,1964.
11. В.К.Прокофьев. Фотографические методы количественного спектрального анализа металлов и сплавов, ч.I. Гостехиздат, 1951.
12. И.А.Гривцев,Г.К.Демьяненко,К.С.Рубцов. ХТФ,т.X,в.I,с.149,1970
13. И.А.Гривцев,И.Н.Гугель,А.Н.Довбня,З.И.Колот,Е.В.Корниенко, Н.И.Мочевников, В.В.Петренко.
    Препринт ФТИ АН УССР, ХФТИ 70-18.

Page 30.

No typing.

END/HT/ST-77-1919.

DISTRIBUTION LIST

DISTRIBUTION DIRECT TO RECIPIENT

ORGANIZATION		MICROFICHE
A205	DMATC	1
A210	DMAAC	2
B344	DIA/RDS-3C	8
C043	USAMIIA	1
C509	BALLISTIC RES LABS	1
C510	AIR MOBILITY R&D LAB/FIO	1
C513	PICATINNY ARSENAL	1
C535	AVIATION SYS COMD	1
[redacted]		[redacted]
C591	FSTC	5
C619	MIA REDSTONE	1
D008	NISC	1
H300	USAICE (USAREUR)	1
P005	ERDA	1
P055	CIA/CRS/ADD/SD	1
NAVORDSTA (50L)		1
NASA/KSI		1
AFIT/LD		1

ORGANIZATION		MICROFICHE
E053	AF/INAKA	1
E017	AF/ RDXTR-W	1
E404	AEDC	1
E408	AFWL	1
E410	ADTC	1
E413	ESD	2
	FTD	
	CCN	1
	ETID	3
	NIA/PHS	1
	NICD	5